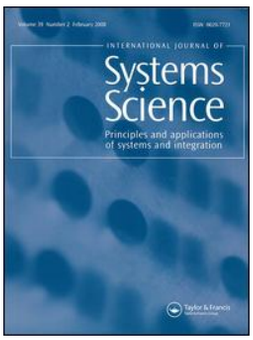

International Journal of Systems Science

ISSN: 0020-7721 (Print) 1464-5319 (Online) Journal homepage: http://www.tandfonline.com/loi/tsys20

# Aerial cooperative transporting and assembling control using multiple quadrotor–manipulator systems

Yuhua Qi, Jianan Wang & Jiayuan Shan

**To cite this article:** Yuhua Qi, Jianan Wang & Jiayuan Shan (2017): Aerial cooperative transporting and assembling control using multiple quadrotor–manipulator systems, International Journal of Systems Science, DOI: 10.1080/00207721.2017.1412538

**To link to this article:** https://doi.org/10.1080/00207721.2017.1412538

Published online: 18 Dec 2017.

Submit your article to this journal

Article views: 24

View related articles

View Crossmark data

Full Terms & Conditions of access and use can be found at
http://www.tandfonline.com/action/journalInformation?journalCode=tsys20

**Download by:** [Beijing Institute of Technology] **Date:** 11 January 2018, At: 19:01

INTERNATIONAL JOURNAL OF SYSTEMS SCIENCE, 2017
https://doi.org/10.1080/00207721.2017.1412538

Taylor & Francis
Taylor & Francis Group

Check for updates

# Aerial cooperative transporting and assembling control using multiple quadrotor–manipulator systems

Yuhua Qi, Jianan Wang and Jiayuan Shan

School of Aerospace Engineering, Beijing Institute of Technology, Beijing, China

**ABSTRACT**

In this paper, a fully distributed control scheme for aerial cooperative transporting and assembling is proposed using multiple quadrotor–manipulator systems with each quadrotor equipped with a robotic manipulator. First, the kinematic and dynamic models of a quadrotor with multi-Degree of Freedom (DOF) robotic manipulator are established together using Euler–Lagrange equations. Based on the aggregated dynamic model, the control scheme consisting of position controller, attitude controller and manipulator controller is presented. Regarding cooperative transporting and assembling, multiple quadrotor–manipulator systems should be able to form a desired formation without collision among quadrotors from any initial position. The desired formation is achieved by the distributed position controller and attitude controller, while the collision avoidance is guaranteed by an artificial potential function method. Then, the transporting and assembling tasks request the manipulators to reach the desired angles cooperatively, which is achieved by the distributed manipulator controller. The overall stability of the closed-loop system is proven by a Lyapunov method and Matrosov's theorem. In the end, the proposed control scheme is simplified for the real application and then validated by two formation flying missions of four quadrotors with 2-DOF manipulators.

**ARTICLE HISTORY**
Received 2 June 2017
Accepted 25 November 2017

**KEYWORDS**
Cooperative control; robotics; collision avoidance; quadrotors; aerial transporting and assembling

Downloaded by [Beijing Institute of Technology] at 19:01 11 January 2018

## 1. Introduction

Nowadays, aerial robots, especially quadrotor–manipulator systems as shown in Figure 1, receive great attention (Arleo, Caccavale, Muscio, & Pierri, 2013; Fumagalli, Naldi, Macchelli, & Forte, 2014; Lee & Kim, 2017; Thomas, Polin, Sreenath, & Kumar, 2013; Yang & Lee, 2014). By combining the mobility of the aerial vehicles with the versatility of robotic manipulator, the application of quadrotor–manipulator systems dramatically expand. Due to the superior mobility of quadrotor, much interest is attracted to utilise them for mobile manipulation such as aerial transportation of payload to locations inaccessible by other means.

Early aerial transportation usually adopted cable lifting for transportation (Michael, Fink, & Kumar, 2011). Obviously, it is limited for further application, i.e. assembling, since the attitude of payload is not controllable. To solve this problem, quadrotors have been equipped with robotic manipulators to enhance the manipulation function. In this case, the dynamics of the robotic manipulator are highly coupled with the quadrotor, which should be carefully considered in the controller design for the overall system. Since quadrotor is an underactuated system, the problem becomes more challenging. Arleo et al. (2013) proposed a hierarchical motion control scheme based on Proportional-Integral-Derivative (PID) controller for the quadrotor–manipulator system to track the desired references. Lee and Kim (2017) presented an online estimation and adaptive control synthesis for an aerial manipulator to carry an unknown payload. In Kim, Choi, and Kim (2013), an adaptive sliding-mode controller is designed for an autonomous flight task including picking up and delivering an object. Two control algorithms were designed in Khalifa, Fanni, Ramadan, and Abo-Ismail (2013) to stabilise the quadrotor and track a desired trajectory under the effect of adding and releasing a payload on the end-effector.

It is well known that a single quadrotor–manipulator system has limited loading capacity. Therefore, it would be even better if multiple quadrotor–manipulator systems with each quadrotor equipped with a robotic manipulator execute a complicated task cooperatively. Compared to the single quadrotor–manipulator system, it can significantly improve the performance of the system and enhance the robustness so that the application field of the overall system would be dramatically expanded. Various research works focus on the cooperative control of the networked Euler–Lagrange (EL) systems (Chung & Slotine, 2009; Qi, Wang, Jia, & Shan, 2016; Ren, 2009)

**CONTACT** Jianan Wang wangjianan@ieee.org
© 2017 Informa UK Limited, trading as Taylor & Francis Group

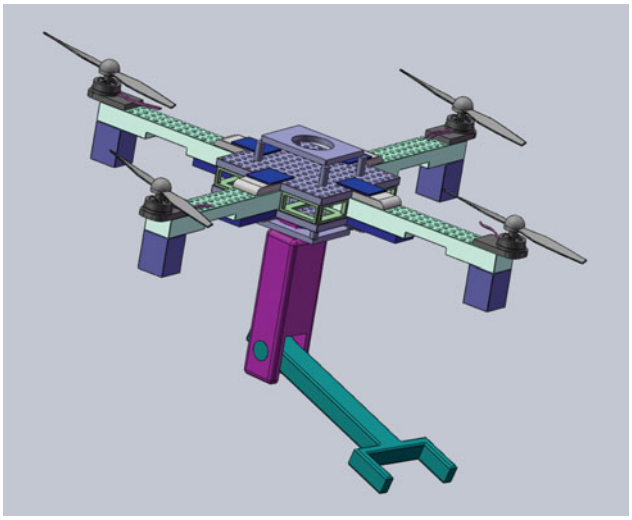

**Figure 1.** A quadrotor equipped with a robotic manipulator.

but very few on the multiple quadrotor–manipulator systems (Gioioso, Franchi, Salvietti, & Scheggi, 2014; Lee, Kim, & Kim, 2016; Mellinger, Shomin, Michael, & Kumar, 2013). Ren (2009) proposed a leaderless consensus algorithm for the multiple EL systems with the conditions of actuator saturation and disturbance. In Chung and Slotine (2009), a synchronisation method of EL system was proposed that can achieve tracking the desired trajectory with a specific topology network. Although the dynamic model of the overall system is in the EL formalism, the above method cannot be applied into the whole system directly because the quadrotor is underactuated. In Mellinger et al. (2013), the problem of controlling multiple quadrotors that cooperatively grasp and transport a payload is considered and individual control laws defined with respect to the payload were presented to stabilise the payload along three-dimensional trajectories. A team of Unmanned Aerial Vehicles (UAVs) grasp an object through a single contact point at the tooltip and transport the object based on a compliant force control method (Gioioso et al., 2014). Lee et al. (2016) presented a motion planning algorithm and an adaptive controller of multiple aerial manipulators for cooperative transportation and the dynamic of the object is also considered. Mellinger et al. (2013), Gioioso et al. (2014), Lee et al. (2016) are in the centralised control fashion, which cannot be directly extended to a large-scale system.

In the scenario of multi-agent systems, collision avoidance is apparently vital for the success of the whole mission. It becomes more severe to avoid collisions in the multiple quadrotor–manipulator systems, especially. Once the collision occurrs, it not only means financial loss but also might cause mission failure. Alonso-Mora, Naegeli, Siegwart, and Beardsley (2015) proposed a path planning method that detects the obstacles and plans a path in the meantime to guarantee collision-free maneuver for the multi-UAV systems. In contrast to path planning methods, real-time collision avoidance strategy computes the avoidance control inputs as obstacles are detected; therefore, it facilitates (in most cases) the treatment of pop-up obstacles. An avoidance control law using a value function to resemble the behaviour of barrier function in the optimisation theory was presented in Dušan, Peter, Mark, and Dragoslav (2007). Hokayem, Stipanović, and Spong (2010) proposed a control law in the presence of bounded disturbances that guarantees collision-free manoeuvres while performing a specific coordination task.

In this paper, the aerial cooperative transporting and assembling control using multiple quadrotor–manipulator systems is considered. The contributions of this paper can be summarised as follows: the general EL dynamic model of the quadrotor equipped with a multi-DOF manipulator is presented handling the quadrotor and the manipulator as an integrated system. The dynamics of the transported components are also considered. Based on the dynamic model of the integrated system, a fully distributed control scheme including position controller, attitude controller and manipulator controller is proposed. The proposed position controller is designed to drive multiple quadrotors to form a desired formation cooperatively and to guarantee collision avoidance which is achieved by an artificial potential function (APF) method. Due to the non-autonomous closed-loop EL equations using the proposed algorithm, the LaSalle's invariance principle is no longer applicable and the convergence analysis is more challenging in this case. Instead, we resort to Matrosov's theorem for convergence analysis of the position controller. The proposed attitude controller is designed for attitude stabilisation of the quadrotor and the proposed manipulator controller is designed via contraction theory to make each manipulator reach the desired joint angles cooperatively. In light of the real application, the proposed control law is further simplified in order to be implementable.

The rest of this paper is organised as follows. In Section 2, we introduce some preliminaries while the kinematic and dynamic models of the integrated system are described in Section 3. In Section 4, the control scheme of the multiple quadrotor–manipulator systems is disscussed as follows: the APF method for collision-free maneuver and the position controller are introduced in Section 4.1, the attitude controller is proposed in Section 4.2 while the manipulator controller is developed in Section 4.3. Two examples of four quadrotor–manipulator systems are presented in Section 5. Finally, Section 6 concludes this paper.

Downloaded by [Beijing Institute of Technology] at 19:01 11 January 2018

Downloaded by [Beijing Institute of Technology] at 19:01 11 January 2018

## 2. Preliminaries

### 2.1. Graph

Weighted undirected graph $\mathcal{G}$ is often used to model communication among $n$-agent systems. Graph $\mathcal{G}$ consists of a node set $\mathcal{V} = \{1, \ldots, n\}$ and an edge set $\mathcal{E} \subseteq \mathcal{V} \times \mathcal{V}$ denoted by a symmetric adjacency matrix $\mathcal{A} = [a_{ij}] \in \mathbb{R}^{n\times n}$ with non-negative adjacency elements $a_{ij}$. Weighted adjacency matrix $\mathcal{A}$ is defined such that $a_{ij} = a_{ji}$ is a positive weight if $(i, j) \in \mathcal{E}$, while $a_{ij} = 0$ if $(i, j) \notin \mathcal{E}$. Let Laplacian matrix $\mathcal{L} = [l_{ij}] \in \mathbb{R}^{n\times n}$ associated with $\mathcal{A}$ be defined as $l_{ii} = \sum_{j=1, j\neq i}^{n} a_{ij}$ and $l_{ij} = -a_{ij}$, where $i \neq j$. Note that $\mathcal{L}$ is symmetric positive semidefinite and $\mathcal{L}$ is positive if and only if $\mathcal{G}$ is connected. Accordingly, if $\mathcal{G}$ is connected and undirected, then $(\mathcal{L} \otimes I_p)\boldsymbol{x} = 0$ or $\boldsymbol{x}^T(\mathcal{L} \otimes I_p) = 0$ if and only if $\boldsymbol{x}_i = \boldsymbol{x}_j$, where $\otimes$ denotes the Kronecker product, $\boldsymbol{x}_i \in \mathbb{R}^p$, $\boldsymbol{x} = [\boldsymbol{x}_1; \ldots; \boldsymbol{x}_n]$. Note that $\boldsymbol{x}^T(\mathcal{L} \otimes I_p)\boldsymbol{x} = \frac{1}{2}\sum_{i=1}^{n}\sum_{j=1}^{n} a_{ij}\|\boldsymbol{x}_i - \boldsymbol{x}_j\|^2$.

### 2.2. Lemma

**Lemma 2.1** [Matrosov's theorem restated in Paden and Panja (1988)]**:** *Given the system*

$$\dot{\boldsymbol{x}} = \boldsymbol{f}(t, \boldsymbol{x}), \tag{1}$$

*where $\boldsymbol{f}(t, \boldsymbol{0}) \equiv \boldsymbol{0}$ and $\boldsymbol{f}$ is such that solutions exist and are unique. Let $V(\boldsymbol{x}, t)$ and $W(\boldsymbol{x}, t)$ be continuous functions on domain $\mathbb{D}$ and satisfying the following four conditions:*

(1) *$V(\boldsymbol{x}, t)$ is positive definite and decrescent.*
(2) *$\dot{V}(\boldsymbol{x}, t) \leq U(\boldsymbol{x}) \leq 0$, where $U(\boldsymbol{x})$ is continuous.*
(3) *$|W(\boldsymbol{x}, t)|$ is bounded.*
(4) *$\max(d(\boldsymbol{x}, \Phi), |\dot{W}(\boldsymbol{x}, t)| \geq \gamma(\|\boldsymbol{x}\|))$, where $\Phi = \{\boldsymbol{x}|U(\boldsymbol{x}) = 0\}$, $d(\boldsymbol{x}, \Phi)$ denotes the distance from $\boldsymbol{x}$ to set $\Phi$, and $\gamma(\cdot)$ is a class $\mathcal{K}$ function.*

*Then, the equilibrium of (1) is uniformly asymptotically stable on $\mathbb{D}$.*

**Lemma 2.2** (Paden & Panja, 1988)**:** *Condition 4 in Lemma 2.1 is satisfied if the following two conditions are satisfied:*

(1) *The function $\dot{W}(\boldsymbol{x}, t)$ is continuous in both arguments and $\dot{W}(\boldsymbol{x}, t) = \boldsymbol{g}(\boldsymbol{x}, \beta(t))$, where $\boldsymbol{g}$ is continuous in both arguments and $\beta(t)$ is continuous and bounded.*
(2) *There exists a class $\mathcal{K}$ function, $\alpha$, such that $|\dot{W}(\boldsymbol{x}, t)| \geq \alpha(\|\boldsymbol{x}\|)$ for all $\boldsymbol{x} \in \Phi$, where $\Phi$ is the set defined in Lemma 2.1.*

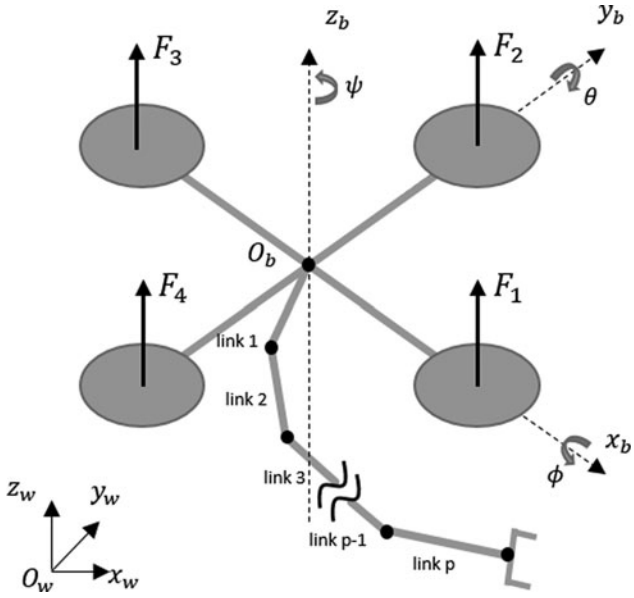


**Figure 2.** The quadrotor–manipulator system with corresponding frames.

## 3. System modelling

In this section, the kinematics and dynamics of the quadrotor–manipulator system are presented in a general version.

### 3.1. Kinematics

Consider a quadrotor–manipulator system consisting of a quadrotor with a $p$-DOF manipulator as shown in Figure 2. Let $\Sigma_w$ denote the world-fixed inertial reference frame, $\Sigma_b$ represent the body-fixed frame of the quadrotor. $\boldsymbol{p}_q = [x; y; z] \in \mathbb{R}^3$ is the position of the mass centre of the quadrotor in $\Sigma_w$. With the roll/pitch/yaw angles of the quadrotor represented by $\boldsymbol{\phi} = [\varphi; \theta; \psi] \in \mathbb{R}^3$, the rotation matrix $R_b$ from $\Sigma_b$ to $\Sigma_w$ is given as

$$R_b = \begin{bmatrix} c_\theta c_\psi - s_\varphi s_\theta s_\psi & -c_\varphi s_\psi & s_\theta c_\psi + s_\varphi c_\theta s_\psi \\ c_\theta s_\psi + s_\varphi s_\theta c_\psi & c_\varphi c_\psi & s_\theta s_\psi - s_\varphi c_\theta c_\psi \\ -c_\varphi s_\theta & s_\varphi & c_\varphi c_\theta \end{bmatrix}, \tag{2}$$

where $c_\gamma$ and $s_\gamma$ denote, respectively, $\cos\gamma$ and $\sin\gamma$. Moreover, let $\dot{\boldsymbol{p}}_q$ denote the absolute linear velocity of the quadrotor and $\boldsymbol{\xi} = [\xi_x; \xi_y; \xi_z] \in \mathbb{R}^3$ denote the absolute angular velocity of the quadrotor which can be represented by $\boldsymbol{\xi} = Q\dot{\boldsymbol{\phi}}$. $Q$ is the transformation matrix between the time derivative of $\boldsymbol{\phi}$ and the absolute angular

Downloaded by [Beijing Institute of Technology] at 19:01 11 January 2018

velocity and is given by

$$Q = \begin{bmatrix} c_\theta & 0 & -c_\varphi s_\theta \\ 0 & 1 & s_\varphi \\ s_\theta & 0 & c_\varphi c_\theta \end{bmatrix}. \tag{3}$$

The generalised state variables of the quadrotor–manipulator system can be given as

$$\boldsymbol{q} = \left[\boldsymbol{p}_q; \boldsymbol{\phi}; \boldsymbol{\alpha}\right] \in \mathbb{R}^{6+p}, \tag{4}$$

where $\boldsymbol{\alpha} = [\alpha_1; \alpha_2; \ldots; \alpha_p] \in \mathbb{R}^p$, $\alpha_i$ is the joint angle of link $i$ of the manipulator. We can easily obtain the kinematics of the quadrotor as follows:

$$\dot{\boldsymbol{p}}_q = [I_{3\times3}, O_{3\times3}, O_{p\times p}]\dot{\boldsymbol{q}}, \tag{5}$$
$$\boldsymbol{\xi} = [O_{3\times3}, Q, O_{p\times p}]\dot{\boldsymbol{q}}, \tag{6}$$

where diag denotes the diagonal matrix, $I_{n\times n}$ is the $n \times n$ identity matrix and $O_{n\times n}$ is the $n \times n$ null matrix.

To express the linear velocity and angular velocity of each link of the manipulator by $\boldsymbol{q}$ and $\dot{\boldsymbol{q}}$, let $\boldsymbol{p}_{l_i}$ denote the position of the mass centre of the link $i$ of the manipulator with respect to $\Sigma_w$ and $\boldsymbol{\xi}_{l_i}$ denote the angular velocity of link $i$ of the manipulator. It is straightforward to obtain

$$\boldsymbol{p}_{l_i} = \boldsymbol{p}_q + R_b \boldsymbol{p}^b_{l_i}, \tag{7}$$
$$\boldsymbol{\xi}_{l_i} = \boldsymbol{\xi} + R_b \boldsymbol{\xi}^b_{l_i}, \tag{8}$$

where $\boldsymbol{p}^b_{l_i}$ is the position of the mass centre of the link $i$ with respect to $\Sigma_b$ and $\boldsymbol{\omega}^b_{l_i}$ is the relative angular velocity between the link $i$ and the frame $\Sigma_b$. According to Siciliano, Sciavicco, Villani, and Oriolo (2010), the following relationship holds:

$$\dot{\boldsymbol{p}}^b_{l_i} = J_{P_i}\dot{\boldsymbol{\alpha}}, \tag{9}$$
$$\boldsymbol{\xi}^b_{l_i} = J_{O_i}\dot{\boldsymbol{\alpha}}, \tag{10}$$

where $J_{P_i}$ and $J_{O_i}$ are the translation and rotation Jacobians, respectively. With Equations (7)–(10), we can obtain

$$\dot{\boldsymbol{p}}_{l_i} = \dot{\boldsymbol{p}}_q - S(R_b \boldsymbol{p}^b_{l_i})\boldsymbol{\xi} + R_b J_{P_i}\dot{\boldsymbol{\alpha}}, \tag{11}$$
$$\boldsymbol{\xi}_{l_i} = \boldsymbol{\xi} + R_b J_{O_i}\dot{\boldsymbol{\alpha}}, \tag{12}$$

where $S(\cdot)$ is the skew-symmetric matrix operator performing the cross product and we apply the fact that $\dot{R}_b = S(\boldsymbol{\xi})R_b$ (Siciliano et al., 2010). With Equations (5), (6), (11) and (12), the translational and angular velocities of the quadrotor and each link of the manipulator in $\Sigma_w$ are mapped by $\boldsymbol{q}$ and $\dot{\boldsymbol{q}}$.

**Remark 3.1:** In the transporting and assembling task, the components will be captured by the robotic manipulators and will have an impact on the dynamics of the quadrotor–manipulator system. In this case, we should consider the dynamics of the components. Due to the low capacity of the quadrotor, we assume the components are light enough to be transported by the quadrotor. When the robotic manipulator captures the component, we assume that the component is firmly grasped by the end-effector. In other words, there is no relative motion between the end-effector and the component. Then, it is easy to obtain

$$\dot{\boldsymbol{p}}_c = \dot{\boldsymbol{p}}_q - S(R_b \boldsymbol{p}^b_c)\boldsymbol{\xi} + R_b J_{P_c}\dot{\boldsymbol{\alpha}}, \tag{13}$$
$$\boldsymbol{\xi}_c = \boldsymbol{\xi} + R_b J_{O_c}\dot{\boldsymbol{\alpha}}. \tag{14}$$

It is easy to find that the kinematics of the component is similar to the kinematics of the manipulator. The component can be viewed as an extra-part of the manipulator. For convenience, we use the subscript $l_{p+1}$ instead of $c$ to represent the component in the following.

### 3.2. Dynamics

To derive the dynamic model of the integrated system, the EL equations are applied as follows:

$$\frac{d}{dt}\frac{\partial L}{\partial \boldsymbol{q}} - \frac{\partial L}{\partial \boldsymbol{q}} = \boldsymbol{u}, \quad L = K - U, \tag{15}$$

where $L$ is the Lagrangian with kinetic energy $K$ and potential energy $U$ of the integrated system and $\boldsymbol{u}$ is the generalised input.

For the quadrotor–manipulator system considered in the previous subsection, the total kinetic energy $K$ and its component are computed as follows:

$$K = K_q + \sum_{i=1}^{p+1} K_{l_i}, \tag{16}$$
$$K_q = \frac{1}{2} m_q \dot{\boldsymbol{p}}_q^T \dot{\boldsymbol{p}}_q + \frac{1}{2}\boldsymbol{\xi}^T R_b I_q R_b^T \boldsymbol{\xi}, \tag{17}$$
$$K_{l_i} = \frac{1}{2} m_{l_i} \dot{\boldsymbol{p}}_{l_i}^T \dot{\boldsymbol{p}}_{l_i} + \frac{1}{2}\boldsymbol{\xi}_{l_i}^T R_b R_{l_i}^b I_{l_i} R_b^{l_i} R_b^T \boldsymbol{\xi}_{l_i}, \tag{18}$$

where $m$ is the mass and $I$ is the inertia matrix. $R^b_{l_i}$ is the rotation matrix from the frame associated to the mass centre of the link $i$ to $\Sigma_b$ and $R_b^{l_i} = (R^b_{l_i})^T$. Likewise, the total potential energy of the integrated system is described as follows:

$$U = U_q + \sum_{i=1}^{p+1} U_{l_i}, \tag{19}$$
$$U_q = m_q g \boldsymbol{e}_3^T \boldsymbol{p}_q, \tag{20}$$

Downloaded by [Beijing Institute of Technology] at 19:01 11 January 2018

$$U_{l_i} = m_{l_i} g \boldsymbol{e}_3^T \left( \boldsymbol{p}_q + R_b \boldsymbol{p}_{l_i}^b \right), \tag{21}$$

where $\boldsymbol{e}_3$ is the unit vector $[\,0\ 0\ 1\,]^T$ and $g$ is the gravity constant.

By substituting (16)–(21) into (15), the dynamic model of the quadrotor–manipulator system can be derived as follows:

$$M(\boldsymbol{q})\ddot{\boldsymbol{q}} + C(\boldsymbol{q}, \dot{\boldsymbol{q}})\dot{\boldsymbol{q}} + G(\boldsymbol{q}) = \boldsymbol{u}, \tag{22}$$

where $M(\boldsymbol{q}) \in \mathbb{R}^{(6+p)\times(6+p)}$ is the symmetric positive-definite inertia matrix. Also, $C(\boldsymbol{q}, \dot{\boldsymbol{q}}) \in \mathbb{R}^{(6+p)\times(6+p)}$ is the Coriolis matrix and $G(\boldsymbol{q}) \in \mathbb{R}^{(6+p)}$ represents gravity effects. Note that we have $\dot{M}(\boldsymbol{q}) - 2C(\boldsymbol{q}, \dot{\boldsymbol{q}})$ is skew-symmetric. The total kinetic energy can be expressed by the inertia matrix $M(\boldsymbol{q})$ as

$$K = \frac{1}{2}\dot{\boldsymbol{q}}^T M(\boldsymbol{q})\dot{\boldsymbol{q}}. \tag{23}$$

By substituting Equations (16)–(20) into (23), the inertia matrix $M(\boldsymbol{q})$ is computed as follows:

$$M(\boldsymbol{q}) = \begin{bmatrix} M_{11} & M_{12} & M_{13} \\ M_{21} & M_{22} & M_{23} \\ M_{31} & M_{32} & M_{33} \end{bmatrix}, \tag{24}$$

$$M_{11} = \left( m_q + \sum_{i=1}^{p+1} m_{l_i} \right) I_{3\times 3}, \tag{25}$$

$$M_{22} = Q^T R_b I_q {R_b}^T Q + \sum_{i=1}^{p} \left( m_{l_i} Q^T S\left(\boldsymbol{p}_{l_i}^b\right)^T S\left(\boldsymbol{p}_{l_i}^b\right) Q + Q^T R_b R_{l_i}^b I_{l_i} \left(R_{l_i}^b\right)^T {R_b}^T Q \right), \tag{26}$$

$$M_{33} = \sum_{i=1}^{p+1} \left( m_{l_i} J_{p_i}^T J_{p_i} + J_{O_i}^T R_{l_i}^b I_{l_i} \left(R_{l_i}^b\right)^T J_{O_i} \right), \tag{27}$$

$$M_{12} = M_{21}^T = -\sum_{i=1}^{p+1} \left( m_{l_i} R_b S\left(\boldsymbol{p}_{l_i}^b\right) Q \right), \tag{28}$$

$$M_{13} = M_{31}^T = \sum_{i=1}^{p+1} \left( m_{l_i} R_b J_{p_i} \right), \tag{29}$$

$$M_{23} = M_{32}^T = \sum_{i=1}^{p+1} \left( Q^T R_b R_{l_i}^b I_{l_i} \left(R_{l_i}^b\right)^T J_{O_i} - m_{l_i} Q^T S\left(\boldsymbol{p}_{l_i}^b\right)^T J_{p_i} \right), \tag{30}$$

where we apply the fact that $RS(\boldsymbol{\xi})R^T = S(R\boldsymbol{\xi})$ if $R$ is a rotation matrix (Siciliano et al., 2010). The Coriolis matrix $C(\boldsymbol{q}, \dot{\boldsymbol{q}})$ can be derived by calculating each element with the following equation (Siciliano et al., 2010):

$$c_{ij} = \sum_{k=1}^{6+\mathrm{p}} \frac{1}{2} \left( \frac{\partial m_{ij}}{\partial q_k} + \frac{\partial m_{ik}}{\partial q_j} - \frac{\partial m_{jk}}{\partial q_i} \right) \dot{q}_k, \tag{31}$$

where $m_{ij}$ is the element of the inertia matrix $M(\boldsymbol{q})$. $G(\boldsymbol{q})$ is calculated with the following partial derivative:

$$G(\boldsymbol{q}) = \frac{\partial U}{\partial \boldsymbol{q}}. \tag{32}$$

We rewrite (22) in the vector form as

$$\begin{bmatrix} M_{11} & M_{12} & M_{13} \\ M_{21} & M_{22} & M_{23} \\ M_{31} & M_{32} & M_{33} \end{bmatrix} \begin{bmatrix} \ddot{\boldsymbol{p}}_q \\ \ddot{\boldsymbol{\phi}} \\ \ddot{\boldsymbol{\alpha}} \end{bmatrix} + \begin{bmatrix} C_{11} & C_{12} & C_{13} \\ C_{21} & C_{22} & C_{23} \\ C_{31} & C_{32} & C_{33} \end{bmatrix} \begin{bmatrix} \dot{\boldsymbol{p}}_q \\ \dot{\boldsymbol{\phi}} \\ \dot{\boldsymbol{\alpha}} \end{bmatrix} + \begin{bmatrix} G_1 \\ G_2 \\ G_3 \end{bmatrix} = \begin{bmatrix} \boldsymbol{u}_f \\ \boldsymbol{u}_\tau \\ \boldsymbol{u}_\alpha \end{bmatrix}, \tag{33}$$

where $\boldsymbol{u}_f$, $\boldsymbol{u}_\tau$, $\boldsymbol{u}_\alpha$ are the generalised inputs corresponding to $\boldsymbol{p}_q$, $\boldsymbol{\phi}$, $\boldsymbol{\alpha}$, respectively. $\boldsymbol{u}_\alpha = [u_{\alpha_1}, \ldots, u_{\alpha_p}]^T \in \mathbb{R}^p$ is the input vector of the manipulator actuation torques which can be actuated directly through joint actuators, such as servo motors. Since the quadrotor is an under-actuated system, $\boldsymbol{u}_f$ and $\boldsymbol{u}_\tau$ need to be transformed to the quadrotor input, $\boldsymbol{F} = [F_1; F_2; F_3; F_4] \in \mathbb{R}^4$, the thrusts of the four motors of the quadrotor. Then, the generalised input can be converted to the inputs of the four motors of the quadrotor and the joint actuators of the manipulator as follows:

$$\begin{bmatrix} \boldsymbol{u}_f \\ \boldsymbol{u}_\tau \\ \boldsymbol{u}_\alpha \end{bmatrix} = \begin{bmatrix} R_b & 0 & 0 \\ 0 & Q^T & 0 \\ 0 & 0 & I_{p\times p} \end{bmatrix} \begin{bmatrix} \Omega & 0 \\ 0 & I_{p\times p} \end{bmatrix} \begin{bmatrix} \boldsymbol{F} \\ \boldsymbol{u}_\alpha \end{bmatrix}, \tag{34}$$

$$\Omega = \begin{bmatrix} 0 & 0 & 0 & 0 \\ 0 & 0 & 0 & 0 \\ 1 & 1 & 1 & 1 \\ 0 & d & 0 & -d \\ -d & 0 & d & 0 \\ c & -c & c & -c \end{bmatrix}, \tag{35}$$

where $d$ is the distance from a motor to the mass centre of the quadrotor and $c$ is the drag factor.

Downloaded by [Beijing Institute of Technology] at 19:01 11 January 2018

## 4. Control scheme

This section depicts the control design method of the quadrotor–manipulator system. Considering $n$ quadrotor–manipulator systems, (22) is represented by

$$M_i(\boldsymbol{q}_i)\ddot{\boldsymbol{q}}_i + C(\boldsymbol{q}_i, \dot{\boldsymbol{q}}_i)\dot{\boldsymbol{q}}_i + G_i(\boldsymbol{q}_i) = \boldsymbol{u}_i,\ i \in N = \{1, \ldots, n\}. \tag{36}$$

For each individual system, the dynamics can be divided into position loop, attitude loop and manipulator loop as follows:

$$M_{11,i}\ddot{\boldsymbol{p}}_i + M_{12,i}\ddot{\boldsymbol{\phi}}_i + M_{13,i}\ddot{\boldsymbol{\alpha}}_i + C_{11,i}\dot{\boldsymbol{p}}_i + C_{12,i}\dot{\boldsymbol{\phi}}_i + C_{13,i}\dot{\boldsymbol{\alpha}}_i + G_{1,i} = \boldsymbol{u}_{f,i}, \tag{37}$$

$$M_{21,i}\ddot{\boldsymbol{p}}_i + M_{22,i}\ddot{\boldsymbol{\phi}}_i + M_{23,i}\ddot{\boldsymbol{\alpha}}_i + C_{21,i}\dot{\boldsymbol{p}}_i + C_{22,i}\dot{\boldsymbol{\phi}}_i + C_{23,i}\dot{\boldsymbol{\alpha}}_i + G_{2,i} = \boldsymbol{u}_{\tau,i}, \tag{38}$$

$$M_{31,i}\ddot{\boldsymbol{p}}_i + M_{32,i}\ddot{\boldsymbol{\phi}}_i + M_{33,i}\ddot{\boldsymbol{\alpha}}_i + C_{31,i}\dot{\boldsymbol{p}}_i + C_{32,i}\dot{\boldsymbol{\phi}}_i + C_{33,i}\dot{\boldsymbol{\alpha}}_i + G_{3,i} = \boldsymbol{u}_{\alpha,i}. \tag{39}$$

where $\boldsymbol{p}_i$ denotes the position of the mass centre of the $i$th quadrotor.

Define the overall avoidance region and the avoidance regions for each pair of quadrotors as

$$\Omega = \bigcup\nolimits_{i,j} \Omega_{ij},\ \Omega_{ij} = \{\boldsymbol{p} : \boldsymbol{p} \in \mathbb{R}^3, \|\boldsymbol{p}_i - \boldsymbol{p}_j\| \le r\}. \tag{40}$$

Also define the overall detection region and the detection regions for each pair of quadrotors as

$$\Psi = \bigcup\nolimits_{i,j} \Psi_{ij},\ \Psi_{ij} = \{\boldsymbol{p} : \boldsymbol{p} \in \mathbb{R}^3, \|\boldsymbol{p}_i - \boldsymbol{p}_j\| \le R\}, \tag{41}$$

where $R > r > 0$, $R$ denotes the radius of the region in which agents can detect the presence of other quadrotors, $r$ denotes the smallest safe distance between the quadrotors.

We assume that each quadrotor–manipulator system is equipped with a sensing device and a communication device. The sensing device can detect other quadrotors if other quadrotors enter the detection region. On the other hand, the communication device is used to communicate between the quadrotors. The aerial cooperative transporting and assembling task of the multiple quadrotor–manipulator systems is divided into three steps: (1) the multiple quadrotor–manipulator systems with the components form a desired formation cooperatively without collision from any initial position, (2) each quadrotor can hover in the air stably and wait for the assembling command and (3) each manipulator can reach a desired joint angle cooperatively to finalise the assembling task.

We present the main result of this paper and the proof follows in three steps.

**Theorem 4.1:** *Consider the multiple quadrotor–manipulator systems (37)–(39) with a ring-structured communication topology. Collision-free transporting and assembling task can be achieved via (45), (64), (70) and (72): (1) $\boldsymbol{p}_i - \boldsymbol{p}_j \to \boldsymbol{\delta}_i - \boldsymbol{\delta}_j$, $\dot{\boldsymbol{p}}_i \to \boldsymbol{0}$, $\forall i \ne j \in N$, (2) $\boldsymbol{\phi}_i \to \boldsymbol{0}$, $\dot{\boldsymbol{\phi}}_i \to \boldsymbol{0}$, $\forall i \in N$ and (3) $\boldsymbol{\alpha}_i \to \boldsymbol{\alpha}_{d,i}$, $\dot{\boldsymbol{\alpha}}_i \to \boldsymbol{0}$, $\forall i \in N$, if $K_{\boldsymbol{p},i} > 0$, $K_{\boldsymbol{\phi},i} > 0$, $K^1_{\boldsymbol{\alpha},i} > 0$, $K^2_{\boldsymbol{\alpha},i} > 0$ and $K^1_{\boldsymbol{\alpha},i} - 2K^2_{\boldsymbol{\alpha},i} > 0$. $\boldsymbol{\delta}_i$ denotes the formation offset of the $i$th quadrotor and $\boldsymbol{\alpha}_{d,i}$ is the desired joint angle of $i$th manipulator.*

### 4.1. Position control

In the position loop, our goal is to guarantee multiple quadrotors forming a formation without collision. To this end, let us define the following avoidance function (Dušan et al., 2007):

$$\mathrm{V}_{ij}(\boldsymbol{p}_i, \boldsymbol{p}_j) = \left(\min\left\{0, \frac{\|\boldsymbol{p}_i - \boldsymbol{p}_j\|^2 - R^2}{\|\boldsymbol{p}_i - \boldsymbol{p}_j\|^2 - r^2}\right\}\right)^2, \quad \forall i \ne j \in N. \tag{42}$$

The partial derivative of $V_{ij}$ with respect to $\boldsymbol{p}_i$ is given by

$$\frac{\partial V_{ij}}{\partial \boldsymbol{p}_i} = \begin{cases} 0 & \|\boldsymbol{p}_i - \boldsymbol{p}_j\| \ge R, \\ 4\dfrac{(R^2 - r^2)(\|\boldsymbol{p}_i - \boldsymbol{p}_j\|^2 - R^2)}{(\|\boldsymbol{p}_i - \boldsymbol{p}_j\|^2 - r^2)^3} \times (\boldsymbol{p}_i - \boldsymbol{p}_j) & R > \|\boldsymbol{p}_i - \boldsymbol{p}_j\| > r, \\ \text{not defined} & \|\boldsymbol{p}_i - \boldsymbol{p}_j\| = r, \\ 0 & \|\boldsymbol{p}_i - \boldsymbol{p}_j\| < r. \end{cases} \tag{43}$$

Since the functions $\mathrm{V}_{ij}(\boldsymbol{p}_i, \boldsymbol{p}_j)$ are symmetric with respect to their arguments, it is easy to obtain

$$\frac{\partial V_{ij}}{\partial \boldsymbol{p}_i} = -\frac{\partial V_{ij}}{\partial \boldsymbol{p}_j} = \frac{\partial V_{ji}}{\partial \boldsymbol{p}_i} = -\frac{\partial V_{ji}}{\partial \boldsymbol{p}_j}. \tag{44}$$

Our goal is to guarantee that the trajectory of each quadrotor avoids the region $\Omega$. To this end, the following position control law is proposed for the $i$th quadrotor–manipulator system:

$$\boldsymbol{u}_{f,i} = M_{12,i}\ddot{\boldsymbol{\phi}}_i + M_{13,i}\ddot{\boldsymbol{\alpha}}_i + C_{12,i}\dot{\boldsymbol{\phi}}_i + C_{13}\dot{\boldsymbol{\alpha}}_i + G_{1,i}$$

Downloaded by [Beijing Institute of Technology] at 19:01 11 January 2018

$$- \sum_{j=1}^{n} \frac{\partial V_{ij}}{\partial \boldsymbol{p}_i} - \sum_{j=1}^{n} a_{ij}[(\boldsymbol{p}_i - \boldsymbol{p}_j) - (\boldsymbol{\delta}_i - \boldsymbol{\delta}_j)] - \sum_{j=1}^{n} b_{ij}\left(\dot{\boldsymbol{p}}_i - \dot{\boldsymbol{p}}_j\right) - K_{\boldsymbol{p},i}\dot{\boldsymbol{p}}_i, \tag{45}$$

where $a_{ij}$ is the $(i, j)$ entry of weighted adjacency matrix $\mathcal{A} \in \mathbb{R}^{n\times n}$ associated with graph $\mathcal{G}_A$ for $q_i$, $b_{ij}$ is the $(i, j)$ entry of weighted adjacency matrix $\mathcal{B} \in \mathbb{R}^{n\times n}$ associated with graph $\mathcal{G}_B$ for $\dot{\boldsymbol{q}}_i$ and $K_{\boldsymbol{p},i} \in \mathbb{R}^{3\times 3}$ is a symmetric matrix. Note that here $\mathcal{G}_A$ and $\mathcal{G}_B$ are allowed to be different.

**Theorem 4.2:** *Given the position loop of the multiple quadrotor–manipulator systems (37), the desired formation can be achieved with collision avoidance under the controller in (43) and (45), i.e. $\boldsymbol{p}_i - \boldsymbol{p}_j \to \boldsymbol{\delta}_i - \boldsymbol{\delta}_j$, $\dot{\boldsymbol{p}}_i \to \boldsymbol{0}$, $\forall i \neq j \in N$ as $t \to \infty$, if graph $\mathcal{G}_A$ and graph $\mathcal{G}_B$ are undirected and connected and $K_{\boldsymbol{p},i} > 0$.*

***Proof:*** Let $\boldsymbol{w}_i = \boldsymbol{p}_i - \boldsymbol{\delta}_i$, $\dot{\boldsymbol{w}}_i = \dot{\boldsymbol{p}}_i - \dot{\boldsymbol{\delta}}_i$, $\boldsymbol{w} = [\boldsymbol{w}_1^T, \ldots, \boldsymbol{w}_n^T]^T$, $\dot{\boldsymbol{w}} = [\dot{\boldsymbol{w}}_1^T, \ldots, \dot{\boldsymbol{w}}_n^T]^T$, $\bar{M}_{11} = \mathrm{diag}[M_{11,1}, \ldots, M_{11,n}]$, $\bar{C}_{11} = \mathrm{diag}[C_{11,1}, \ldots, C_{11,n}]$, $K_{\boldsymbol{p}} = \mathrm{diag}[K_{\boldsymbol{p},1}, \ldots, K_{\boldsymbol{p},n}]$, $\nabla = [\sum_{j=1}^{n} \frac{\partial V_{1j}}{\partial \boldsymbol{p}_1}; \ldots; \sum_{j=1}^{n} \frac{\partial V_{nj}}{\partial \boldsymbol{p}_n}]$. Using (45), (37) can be written in vector form as

$$\bar{M}_{11}\dot{\boldsymbol{w}} + \bar{C}_{11}\dot{\boldsymbol{w}} = -(\mathcal{L}_A \otimes I_{3\times 3})\boldsymbol{w} - (\mathcal{L}_B \otimes I_{3\times 3})\dot{\boldsymbol{w}} - K_{\boldsymbol{p}}\dot{\boldsymbol{w}} - \nabla, \tag{46}$$

where $\mathcal{L}_A$, $\mathcal{L}_B$ are the Laplacian matrices associated with $\mathcal{G}_A$ and $\mathcal{G}_B$, respectively. Using (45), (37) can also written as

$$\frac{d}{dt}(\boldsymbol{w}_i - \boldsymbol{w}_j) = \dot{\boldsymbol{w}}_i - \dot{\boldsymbol{w}}_j, \tag{47}$$

$$\frac{d}{dt}\dot{\boldsymbol{w}}_i = -M_{11,i}^{-1}\left[C_{11,i}\dot{\boldsymbol{w}}_i + \sum_{j=1}^{n} a_{ij}(\boldsymbol{w}_i - \boldsymbol{w}_j) + \sum_{j=1}^{n} b_{ij}\left(\dot{\boldsymbol{w}}_i - \dot{\boldsymbol{w}}_j\right) + K_{\boldsymbol{p},i}\dot{\boldsymbol{w}}_i + \sum_{j=1}^{n} \frac{\partial V_{ij}}{\partial \boldsymbol{p}_i}\right]. \tag{48}$$

Let $\tilde{\boldsymbol{w}}$ be a column stack vector of all $\boldsymbol{w}_i - \boldsymbol{w}_j$, where $i < j$ and $a_{ij} \neq 0$. Consider a Lyapunov function candidate for (47) and (48) as

$$V_1 = \frac{1}{2}\boldsymbol{w}^T(\mathcal{L}_A \otimes I_{3\times 3})\boldsymbol{w} + \frac{1}{2}\dot{\boldsymbol{w}}^T\bar{M}_{11}\dot{\boldsymbol{w}} + \sum_{i=1}^{n}\sum_{j>i} V_{ij}. \tag{49}$$

Because $\boldsymbol{w}^T(\mathcal{L}_A \otimes I_{3\times 3})\boldsymbol{w} = \frac{1}{2}\sum_{i=1}^{n}\sum_{j=1}^{n} a_{ij}\|\boldsymbol{w}_i - \boldsymbol{w}_j\|^2$, $V_1$ is positive definite and decrescent with respect to $\tilde{\boldsymbol{w}}$ and $\dot{\boldsymbol{w}}$. Note that system (47) and (48) is non-autonomous due to the dependence of $M_{11,i}$ and $C_{11,i}$ on $\boldsymbol{q}_i$. As a result, LaSalle's invariance principle is no longer applicable for (47) and (48). Instead, we apply Matrosov's theorem in Lemma 2.1 to prove the theorem. Note that Condition (1) in Lemma 2.1 is satisfied.

The derivative of $V_1$ with respect to $t$ is given by

$$\dot{V}_1 = \dot{\boldsymbol{w}}^T(\mathcal{L}_A \otimes I_{3\times 3})\boldsymbol{w} + \dot{\boldsymbol{w}}^T\bar{M}_{11}\dot{\boldsymbol{w}} + \frac{1}{2}\dot{\boldsymbol{w}}^T\dot{\bar{M}}_{11}\dot{\boldsymbol{w}} + \sum_{i=1}^{n}\sum_{j>i}\left(\left(\frac{\partial V_{ij}}{\partial \boldsymbol{p}_i}\right)^T\dot{\boldsymbol{p}}_i + \left(\frac{\partial V_{ij}}{\partial \boldsymbol{p}_j}\right)^T\dot{\boldsymbol{p}}_j\right). \tag{50}$$

Applying (46) yields,

$$\dot{V}_1 = \dot{\boldsymbol{w}}^T(\mathcal{L}_A \otimes I_{3\times 3})\boldsymbol{w} + \dot{\boldsymbol{w}}^T\left[-\bar{C}_{11}\dot{\boldsymbol{w}} - (\mathcal{L}_A \otimes I_{3\times 3})\boldsymbol{w} - (\mathcal{L}_B \otimes I_{3\times 3})\dot{\boldsymbol{w}} - K_{\boldsymbol{p}}\dot{\boldsymbol{w}} - \nabla\right] + \frac{1}{2}\dot{\boldsymbol{w}}^T\dot{\bar{M}}_{11}\dot{\boldsymbol{w}} + \sum_{i=1}^{n}\sum_{j>i}\left(\left(\frac{\partial V_{ij}}{\partial \boldsymbol{p}_i}\right)^T\dot{\boldsymbol{p}}_i + \left(\frac{\partial V_{ij}}{\partial \boldsymbol{p}_j}\right)^T\dot{\boldsymbol{p}}_j\right). \tag{51}$$

Note that $\dot{\bar{M}}_{11} - 2\bar{C}_{11}$ is skew symmetric.

$$\dot{V}_1 = -\dot{\boldsymbol{w}}^T(\mathcal{L}_B \otimes I_{3\times 3})\dot{\boldsymbol{w}} - \dot{\boldsymbol{w}}^T K_{\boldsymbol{p}}\dot{\boldsymbol{w}} - \dot{\boldsymbol{w}}^T\nabla + \sum_{i=1}^{n}\sum_{j>i}\left(\left(\frac{\partial V_{ij}}{\partial \boldsymbol{p}_i}\right)^T\dot{\boldsymbol{p}}_i + \left(\frac{\partial V_{ij}}{\partial \boldsymbol{p}_j}\right)^T\dot{\boldsymbol{p}}_j\right), \tag{52}$$

$$\dot{V}_1 = -\dot{\boldsymbol{w}}^T(\mathcal{L}_B \otimes I_{3\times 3})\dot{\boldsymbol{w}} - \dot{\boldsymbol{w}}^T K_{\boldsymbol{p}}\dot{\boldsymbol{w}} - \sum_{i=1}^{n}\sum_{j=1}^{n}\dot{\boldsymbol{p}}_i^T\frac{\partial V_{ij}}{\partial \boldsymbol{p}_i} + \sum_{i=1}^{n}\sum_{j>i}\left(\left(\frac{\partial V_{ij}}{\partial \boldsymbol{p}_i}\right)^T\dot{\boldsymbol{p}}_i + \left(\frac{\partial V_{ij}}{\partial \boldsymbol{p}_j}\right)^T\dot{\boldsymbol{p}}_j\right). \tag{53}$$

Using Equation (44),

$$-\sum_{i=1}^{n}\sum_{j=1}^{n}\dot{\boldsymbol{p}}_i^T\frac{\partial V_{ij}}{\partial \boldsymbol{p}_i} + \sum_{i=1}^{n}\sum_{j>i}\left(\left(\frac{\partial V_{ij}}{\partial \boldsymbol{p}_i}\right)^T\dot{\boldsymbol{p}}_i + \left(\frac{\partial V_{ij}}{\partial \boldsymbol{p}_j}\right)^T\dot{\boldsymbol{p}}_j\right) = 0. \tag{54}$$

Then,

$$\dot{V}_1 = -\dot{\boldsymbol{w}}^T(\mathcal{L}_B \otimes I_{3\times 3})\dot{\boldsymbol{w}} - \dot{\boldsymbol{w}}^T K_{\boldsymbol{p}}\dot{\boldsymbol{w}} \leq 0, \tag{55}$$

where we apply the fact that $-\dot{\boldsymbol{w}}^T(\mathcal{L}_B \otimes I_{3\times 3})\dot{\boldsymbol{w}} \leq 0$ because graph $\mathcal{G}_B$ is undirected and $K_{\boldsymbol{p}} > 0$ because $K_{\boldsymbol{p},i} > 0$. Therefore, Condition (2) in Lemma 2.1 is satisfied.

Note that (55) implies that $V_1(t) \leq V_1(0)$, $\forall t \geq 0$ and (42) implies that $\lim_{\|\boldsymbol{p}_i - \boldsymbol{p}_j\| \to r^+} V_{ij}(\boldsymbol{p}_i, \boldsymbol{p}_j) = \infty \quad \forall i, j.$

Downloaded by [Beijing Institute of Technology] at 19:01 11 January 2018

We conclude that the trajectory of the quadrotors will never enter $\Omega$ and hence collisions are avoided.

Let $W = \dot{\boldsymbol{w}}^T \bar{M}_{11}(\mathcal{L}_A \otimes I_{3\times 3})\boldsymbol{w}$. Then, we have

$$|W| < \|\dot{\boldsymbol{w}}\| \left\|\bar{M}_{11}\right\| \|(\mathcal{L}_A \otimes I_{3\times 3})\boldsymbol{w}\|. \tag{56}$$

According to (25), $\|\bar{M}_{11}\|$ is bounded. Because $V_1(t) \le V_1(0)$, $\forall t \ge 0$, $\tilde{\boldsymbol{w}}$ and $\|\dot{\boldsymbol{w}}\|$ are bounded. Noting that $(\mathcal{L}_A \otimes I_{3\times 3})\boldsymbol{w}$ is a column stack vector of all $\sum_{j=1}^{n} a_{ij}(\boldsymbol{w}_i - \boldsymbol{w}_j)$, $i = 1, \ldots, n$, it follows that $\|(\mathcal{L}_A \otimes I_{3\times 3})\boldsymbol{w}\|$ is also bounded. Then, it thus follows that $|W|$ is bounded along the solution trajectory, implying that Condition (3) in Lemma 2.1 is satisfied. The derivative of $W$ along the solution trajectory of (47) and (48) is

$$\begin{aligned}\dot{W} = {} & \ddot{\boldsymbol{w}}^T \bar{M}_{11}(\mathcal{L}_A \otimes I_{3\times 3})\boldsymbol{w} + \dot{\boldsymbol{w}}^T \dot{\bar{M}}_{11}(\mathcal{L}_A \otimes I_{3\times 3})\boldsymbol{w} \\ & + \dot{\boldsymbol{w}}^T \bar{M}_{11}(\mathcal{L}_A \otimes I_{3\times 3})\dot{\boldsymbol{w}},\end{aligned} \tag{57}$$

$$\begin{aligned}\dot{W} = {} & -\dot{\boldsymbol{w}}^T \bar{C}_{11}^T(\mathcal{L}_A \otimes I_{3\times 3})\boldsymbol{w} - \boldsymbol{w}^T(\mathcal{L}_A^2 \otimes I_{3\times 3})\boldsymbol{w} \\ & - \dot{\boldsymbol{w}}^T(\mathcal{L}_B\mathcal{L}_A \otimes I_{3\times 3})\boldsymbol{w} - \dot{\boldsymbol{w}}^T K_{\boldsymbol{p}}(\mathcal{L}_A \otimes I_{3\times 3})\boldsymbol{w} \\ & - \nabla^T(\mathcal{L}_A \otimes I_{3\times 3})\boldsymbol{w} + \dot{\boldsymbol{w}}^T \dot{\bar{M}}_{11}(\mathcal{L}_A \otimes I_{3\times 3})\boldsymbol{w} \\ & + \dot{\boldsymbol{w}}^T \bar{M}_{11}(\mathcal{L}_A \otimes I_{3\times 3})\dot{\boldsymbol{w}},\end{aligned} \tag{58}$$

where we apply the property of the Kronecker products in Graham (1982). Note that $\dot{V}_1 = 0$ implies $\dot{\boldsymbol{w}} = 0$. On the set $\{(\tilde{\boldsymbol{w}}, \dot{\boldsymbol{w}}) | \dot{V}_1 = 0\}$, we have

$$\dot{W} = -\boldsymbol{w}^T(\mathcal{L}_A^2 \otimes I_{3\times 3})\boldsymbol{w} \le 0. \tag{59}$$

Note that $|\dot{W}| = \|(\mathcal{L}_A^2 \otimes I_{3\times 3})\boldsymbol{w}\|^2$ is positive definite with respect to $\tilde{\boldsymbol{w}}$. Therefore, there exists a class $\mathcal{K}$ function, $\alpha$, such that $|\dot{W}| > \alpha(\|\tilde{\boldsymbol{w}}\|)$ (Khalil (1996)). Also, note that $|\dot{W}|$ does not explicitly depend on $t$. It follows from Lemma 2.2 that Condition (4) in Lemma 2.1 is satisfied. In conclusion, the equilibrium of system (47) and (48) is uniformly asymptotically stable, which implies that $\boldsymbol{p}_i - \boldsymbol{p}_j \to \boldsymbol{\delta}_i - \boldsymbol{\delta}_j$, $\dot{\boldsymbol{p}}_i \to \boldsymbol{0}$ as $t \to \infty$ and the region $\Omega$ is avoidable. □

### 4.2. Attitude control

Next, $\boldsymbol{u}_\tau$ is designed to achieve the desired attitude of the quadrotor. According to (34), $\boldsymbol{u}_f$ depends on the attitude of the quadrotor via the relation

$$\begin{bmatrix} u_{f,x} \\ u_{f,y} \\ u_{f,z} \end{bmatrix} = \begin{bmatrix} (\cos\psi\sin\theta\cos\varphi + \sin\psi\sin\varphi) f_z \\ (\sin\psi\sin\theta\cos\varphi - \cos\psi\sin\varphi) f_z \\ \cos\theta\cos\varphi f_z \end{bmatrix}, \tag{60}$$

where $f_z = \|\boldsymbol{u}_f\|$ is the total thrust of the quadrotor with respect to $\Sigma_b$. Therefore, the reference state for the roll and pitch angles can be computed as

$$\varphi_d = \arctan\left(\frac{u_{f,x}\cos\psi + u_{f,y}\sin\psi}{u_{f,z}}\right), \tag{61}$$

$$\theta_d = \arcsin\left(\frac{u_{f,x}\sin\psi - u_{f,y}\cos\psi}{\|\boldsymbol{u}_f\|}\right). \tag{62}$$

**Remark 4.1:** According to (61) and (62), $\varphi_d$ and $\theta_d$ are calculated by the input of the position loop. When the quadrotors arrive at the desired position, or $u_{f,x} = u_{f,y} = 0$, then $\varphi_d = \theta_d = 0$. On the other hand, we always choose $\psi_d = 0$.

Define the auxiliary variables as follows:

$$\boldsymbol{s}_{\phi,i} = \dot{\boldsymbol{\phi}}_i - \dot{\boldsymbol{\phi}}_{r,i}, \ \dot{\boldsymbol{\phi}}_{r,i} = -\Lambda_\phi(\boldsymbol{\phi}_i - \boldsymbol{\phi}_{d,i}), \tag{63}$$

where $\Lambda_\phi \in \mathbb{R}^{3\times 3}$ is a positive matrix and $\boldsymbol{\phi}_{d,i} = [\varphi_{d,i}; \theta_{d,i}; \psi_{d,i}]$.

Then, the attitude control law is proposed for the $i$th quadrotor–manipulator system as follows:

$$\begin{aligned}\boldsymbol{u}_{\tau,i} = {} & M_{21,i}\ddot{\boldsymbol{p}}_i + M_{23,i}\ddot{\boldsymbol{\alpha}}_i + C_{21,i}\dot{\boldsymbol{p}}_i + C_{23}\dot{\boldsymbol{\alpha}}_i + G_{2,i} \\ & + M_{22,i}\ddot{\boldsymbol{\phi}}_{r,i} + C_{22,i}\dot{\boldsymbol{\phi}}_{r,i} - K_{\boldsymbol{\phi},i}\boldsymbol{s}_{\phi,i},\end{aligned} \tag{64}$$

where $K_{\boldsymbol{\phi},i} \in \mathbb{R}^{3\times 3}$ is a diagonal matrix.

**Theorem 4.3:** *Consider the system (38) with (64), the desired attitude can be achieved, i.e. $\boldsymbol{\phi}_i \to \boldsymbol{\phi}_{d,i}$, $\dot{\boldsymbol{\phi}}_i \to \boldsymbol{0}$, $\forall i \in N$ as $t \to \infty$, if $K_{\boldsymbol{\phi},i} > 0$.*

***Proof:*** Using (64), (38) can be rewritten as

$$M_{22,i}\dot{\boldsymbol{s}}_{\phi,i} + C_{22,i}\boldsymbol{s}_{\phi,i} + K_\phi \boldsymbol{s}_{\phi,i} = 0. \tag{65}$$

Choose a Lyapunov function candidate for (38) as

$$V_2 = \frac{1}{2}\boldsymbol{s}_{\phi,i}{}^T M_{22,i}\boldsymbol{s}_{\phi,i}. \tag{66}$$

Then, the derivative of $V$ is given by

$$\dot{V}_2 = \boldsymbol{s}_{\phi,i}{}^T M_{22,i}\dot{\boldsymbol{s}}_{\phi,i} + \frac{1}{2}\boldsymbol{s}_{\phi,i}{}^T \dot{M}_{22,i}\boldsymbol{s}_{\phi,i}. \tag{67}$$

By applying (65),

$$\dot{V}_2 = \boldsymbol{s}_{\phi,i}{}^T(-C_{22,i}\boldsymbol{s}_{\phi,i} - K_{\boldsymbol{\phi},i}\boldsymbol{s}_{\phi,i}) + \frac{1}{2}\boldsymbol{s}_\phi{}^T \dot{M}_{22}\boldsymbol{s}_\phi, \tag{68}$$

$$\dot{V}_2 = -\boldsymbol{s}_{\phi,i}^T K_{\boldsymbol{\phi},i}\boldsymbol{s}_{\phi,i} < 0, \tag{69}$$

where we apply the fact that $\dot{M}_{22,i} - 2C_{22,i}$ is skew symmetric. It implies that $\boldsymbol{s}_{\phi,i} \to 0$ as $t \to \infty$, which means $\phi_i \to \phi_{d,i}$, $\dot{\phi}_i \to \mathbf{0}$ as $t \to \infty$. □

**Remark 4.2:** According to (34) and (35), the real quadrotor input can be given as follows:

$$\boldsymbol{F} = \Omega^{+} \begin{bmatrix} R_b^{-1} & 0 \\ 0 & Q^{-T} \end{bmatrix} \begin{bmatrix} \boldsymbol{u}_f \\ \boldsymbol{u}_\tau \end{bmatrix}, \tag{70}$$

where $\Omega^{+}$ denotes the Moore–Penrose pseudoinverse of matrix $\Omega$. $\boldsymbol{u}_f$ and $\boldsymbol{u}_\tau$ are given in (45) and (64).

### 4.3. Manipulator control

Finally, $\boldsymbol{u}_\alpha$ is designed to cooperatively track the desired joint angles for the manipulators. Define the auxiliary variables as follows:

$$\boldsymbol{s}_{\alpha,i} = \dot{\boldsymbol{\alpha}}_i - \dot{\boldsymbol{\alpha}}_{r,i}, \ \dot{\boldsymbol{\alpha}}_{r,i} = -\Lambda_\alpha(\boldsymbol{\alpha}_i - \boldsymbol{\alpha}_{d,i}), \tag{71}$$

where $\Lambda_\alpha \in \mathbb{R}^{p\times p}$ is positive and $\boldsymbol{\alpha}_{d,i} = [\alpha_{1d,i}; \ldots; \alpha_{pd,i}]$.

Then, the manipulator control law is proposed for the $i$th quadrotor–manipulator system as follows:

$$\begin{aligned} \boldsymbol{u}_{\alpha,i} = {} & M_{31,i}\ddot{\boldsymbol{p}}_i + M_{32,i}\ddot{\boldsymbol{\phi}}_i + C_{31,i}\dot{\boldsymbol{p}}_i + C_{32}\dot{\boldsymbol{\phi}}_i + G_{3,i} + M_{33,i}\ddot{\boldsymbol{\alpha}}_{r,i} \\ & + C_{33,i}\dot{\boldsymbol{\alpha}}_{r,i} - K^1_{\alpha,i}\boldsymbol{s}_{\alpha,i} + K^2_{\alpha,i}\boldsymbol{s}_{\alpha,i-1} + K^2_{\alpha,i}\boldsymbol{s}_{\alpha,i+1}, \end{aligned} \tag{72}$$

where $K^1_{\alpha,i} \in \mathbb{R}^{p\times p}$ is a feedback gain for the $i$th manipulator and $K^2_{\alpha,i} \in \mathbb{R}^{p\times p}$ is a coupling gain with the adjacent members ($i-1$ and $i+1$).

**Remark 4.3:** From control law (72), the $i$th robotic manipulator only can receive information from the adjacent manipulators (*i-1* and *i + 1*). In this paper, a two-way ring-structured communication topology is adopted for the whole multiple quadrotor–manipulator systems, which also guarantees that graph $\mathcal{G}_A$ and graph $\mathcal{G}_B$ are undirected and connected.

**Theorem 4.4:** *Consider the system (39) with (72) in a ring-structured communication topology,* $\boldsymbol{\alpha}_i \to \boldsymbol{\alpha}_{d,i}$, $\dot{\boldsymbol{\alpha}}_i \to \mathbf{0}$, $\forall i \in N$ *as* $t \to \infty$, *if* $K^1_{\alpha,i} > 0$, $K^2_{\alpha,i} > 0$ *and* $K^1_{\alpha,i} - 2K^2_{\alpha,i} > 0$.

***Proof:*** The closed-loop system after applying the manipulator controller (72) to (39) can be written as follows:

$$M_{33,i}\dot{\boldsymbol{s}}_{\alpha,i} + C_{33,i}\boldsymbol{s}_{\alpha,i} + K^1_{\alpha,i}\boldsymbol{s}_{\alpha,i} - K^2_{\alpha,i}\boldsymbol{s}_{\alpha,i-1} - K^2_{\alpha,i}\boldsymbol{s}_{\alpha,i+1} = 0. \tag{73}$$

The following proof is the same as in Qi et al. (2016). □

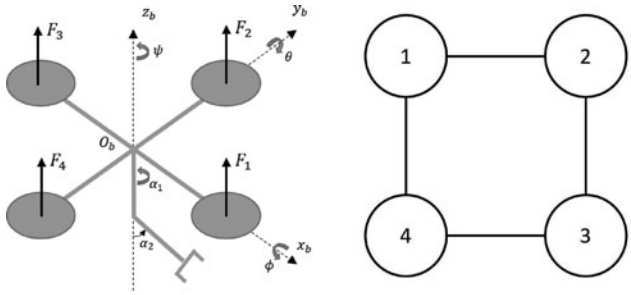


(a) Quadrotor-manipulator system. (b) Communication topology.

**Figure 3.** The quadrotor–manipulator system and communication topology used in simulation.

**Table 1.** Physical parameters.

| | |
|---|---|
| Mass of quadrotor $m_q$ | 1 kg |
| Length of quadrotor arm $l_q$ | 0.4 m |
| Inertia matrix of quadrotor $I_q$ | [1,1,2.48] |
| Mass of link $j$ of manipulator [$m_1$, $m_2$] | [0.3,0.3] kg |
| Length of link $j$ of manipulator [$l_1$, $l_2$] | [0.3,0.5] m |
| Radius of the link 1 $r$ | 0.03 m |

## 5. Simulation

The proposed control scheme in the previous section will be verified using Matlab. We consider four identical quadrotor–manipulator systems with each quadrotor equipped with a 2-DOF manipulator as shown in Figure 3(a). Link 1 of the manipulator is attached to the bottom of the quadrotor and can move along the direction of angle $\alpha_1$. Link 2 of the manipulator, connecting link 1 and the end-effector, can move along the direction of angle $\alpha_2$. The two-way ring network structure for the four quadrotor–manipulator systems is shown in Figure 3(b). The physical parameters of the integrated system are given in Table 1.

The translation and rotation Jacobians of the quadrotor–manipulator system are given as follows:

$$J_{P_1} = O_{3\times 3}, \quad J_{P_2} = \begin{bmatrix} -\frac{1}{2}l_2\sin(\alpha_1)\sin(\alpha_2) & \frac{1}{2}l_2\cos(\alpha_1)\cos(\alpha_2) \\ \frac{1}{2}l_2\cos(\alpha_1)\sin(\alpha_2) & \frac{1}{2}l_2\sin(\alpha_1)\cos(\alpha_2) \\ 0 & \frac{1}{2}l_2\sin(\alpha_2) \end{bmatrix}, \tag{74}$$

$$J_{O_1} = \begin{bmatrix} 0 & 0 & 1 \\ 0 & 0 & 0 \end{bmatrix}, \quad J_{O_2} = J_{O_1} + R^b_{l_1}\begin{bmatrix} 0 & 0 & 0 \\ 0 & -1 & 0 \end{bmatrix}. \tag{75}$$

In the real application, it is difficult to measure the acceleration information, e.g. $\ddot{\boldsymbol{p}}$, $\ddot{\boldsymbol{\phi}}$ and $\ddot{\boldsymbol{\alpha}}$. On the other hand, the manipulator links are much lighter than the quadrotor body. Due to Equations (25)–(30), the elements of matrix $M_{12,i}$ and $M_{13,i}$ are often negligible with

Downloaded by [Beijing Institute of Technology] at 19:01 11 January 2018

respect to $M_{11,i}$. Therefore, in practice, $u_{f,i}$ in (76) is very close to the ideal control input in (45). Hence, we rewrite the controller (45), (64) and (72) as follows:

$$\boldsymbol{u}_{f,i} = C_{12,i}\dot{\phi}_i + C_{13}\dot{\boldsymbol{\alpha}}_i + G_{1,i} - \sum_{j=1}^{n} \frac{\partial V_{ij}}{\partial \boldsymbol{p}_i} - K_{\boldsymbol{p},i}\dot{\boldsymbol{p}}_i - \sum_{j=1}^{n} a_{ij}[(\boldsymbol{p}_i - \boldsymbol{p}_j) - (\boldsymbol{\delta}_i - \boldsymbol{\delta}_j)] - \sum_{j=1}^{n} b_{ij}\left(\dot{\boldsymbol{p}}_i - \dot{\boldsymbol{p}}_j\right), \tag{76}$$

$$\boldsymbol{u}_{\tau,i} = C_{21,i}\dot{\boldsymbol{p}}_i + C_{23}\dot{\boldsymbol{\alpha}}_i + G_{2,i} + M_{22,i}\ddot{\phi}_{r,i} + C_{22,i}\dot{\phi}_{r,i} - K_{\phi}\boldsymbol{s}_{\phi,i}, \tag{77}$$

$$\boldsymbol{u}_{\alpha,i} = C_{31,i}\dot{\boldsymbol{p}}_i + C_{32}\dot{\phi}_i + G_{3,i} + M_{33,i}\ddot{\boldsymbol{\alpha}}_{r,i} + C_{33,i}\dot{\boldsymbol{\alpha}}_{r,i} - K^1_{\alpha,i}\boldsymbol{s}_{\alpha,i} + K^2_{\alpha,i}\boldsymbol{s}_{\alpha,i-1} + K^2_{\alpha,i}\boldsymbol{s}_{\alpha,i+1}. \tag{78}$$

In this section, we present two examples to illustrate the performance of the control scheme. In the first example, a transporting task of four quadrotor–manipulator systems is presented to show the effectiveness of the APF. In the second one, a transporting and assembling task of four quadrotor–manipulator systems is presented to demonstrate the performance of the proposed controller.

### 5.1. Example 1 – transporting task

Let us consider that four quadrotors hover at the vertices of a virtual 5-m high rhombus with coordinates [−15, 0, 5], [15, 0.5, 5], [0.5, −15, 5] and [0, 15, 5] m. The desired formation is also a rhombus but each quadrotor needs to fly to the opposite vertex of the rhombus. In this simulation, we choose $R = 8$ m, $r = 2$ m and the formation offset vectors are designed as $\delta_1 = [10, 0, 0]$ m, $\delta_2 = [-10, 0, 0]$ m, $\delta_3 = [0, 10, 0]$ m and $\delta_4 = [0, -10, 0]$ m. The desired angles of the manipulator are $\alpha_{d,i} = [0, 0]^T$ rad for $\forall i \in N$.

The simulation results are presented in Figures 4–10. For the control gains in Equations (76)–(78), we choose $K_{p,i} = \text{diag}[5, 5, 5]$, $K_{\phi,i} = \text{diag}[10, 10, 10]$, $\Lambda_{\phi} = \text{diag}[20, 20, 20]$, $K^1_{\alpha,i} = \text{diag}[5, 5]$, $K^2_{\alpha,i} = \text{diag}[2, 2]$ and $\Lambda_{\alpha} = \text{diag}[10, 10, 10]$ for each quadrotor–manipulator system. Figure 4 shows the trajectories of four quadrotors in the $X$–$Y$ plane. Square represents the initial position of the quadrotor and circle represents the terminal position of the quadrotor. In Figure 4, the quadrotors move in straight lines at the beginning. When they detect each other at the boundary of the detection regions, they change their directions to avoid collisions and then achieve the final formation. Figure 5 shows the relative

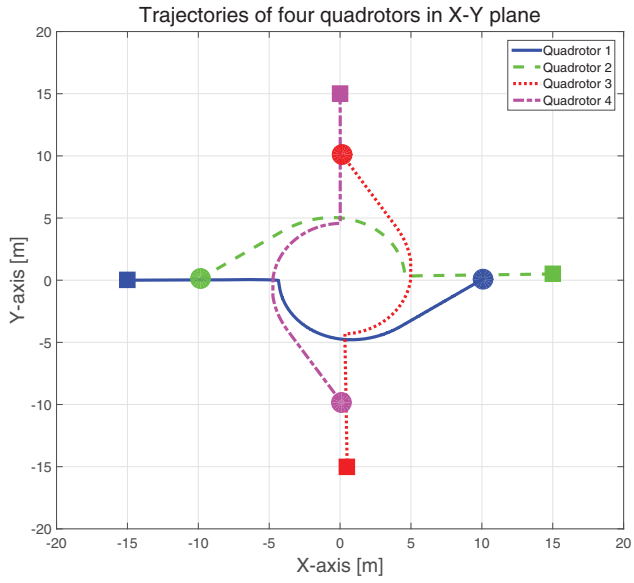


**Figure 4.** Planar trajectory.

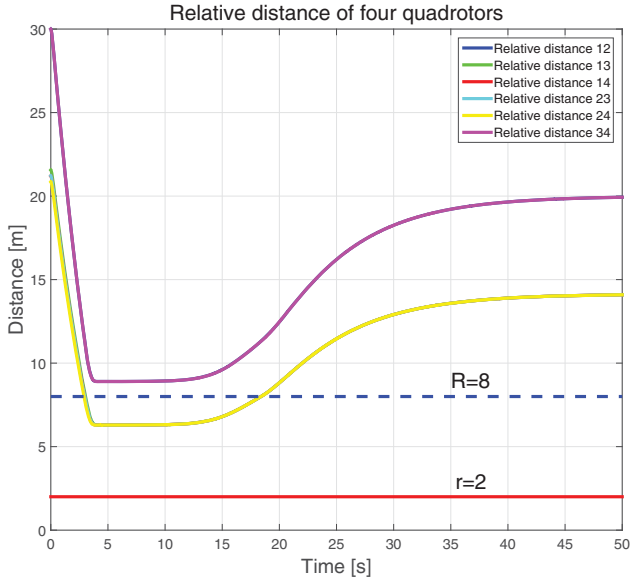


**Figure 5.** Relative distance.

distances of the four quadrotors. It can be seen that when quadrotors enter the detection region, a repulsive force appears to make the quadrotor fly away from the detection region. Therefore, the inter-agent distances are always larger than the smallest safe distance $r$. Hence, collisions are avoided between quadrotors. Figure 6 shows the positions history of the four quadrotors in the $X$, $Y$, $Z$-axes. The quadrotors stop and the formation is formed when $t$ is greater than 40 s. Figure 7 shows the Euler angles history of the four quadrotors. The repulsive forces are generated by corresponding attitudes of quadrotors at the time instants when collisions are

Downloaded by [Beijing Institute of Technology] at 19:01 11 January 2018

Downloaded by [Beijing Institute of Technology] at 19:01 11 January 2018

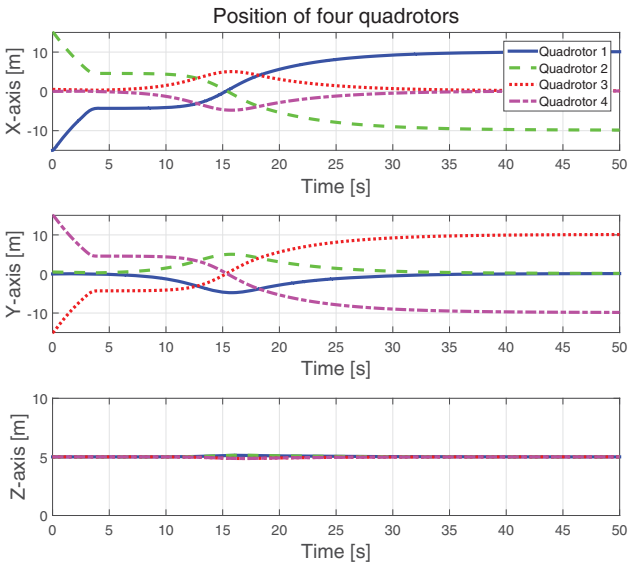


**Figure 6.** Positions of the four quadrotors.

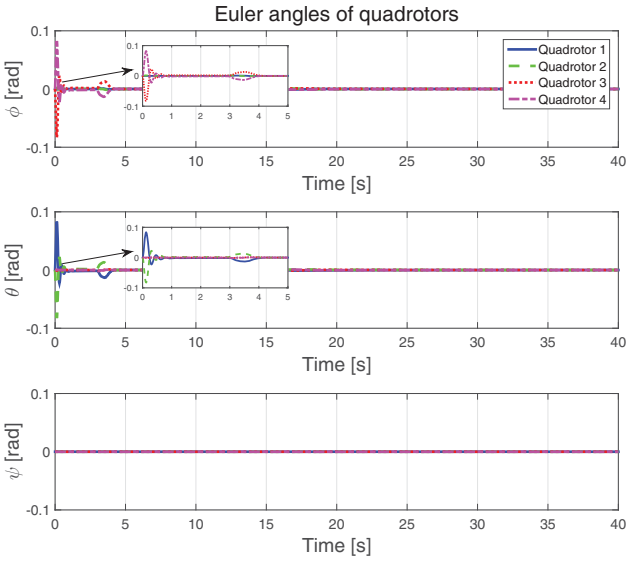


**Figure 7.** Euler angles of the four quadrotors.

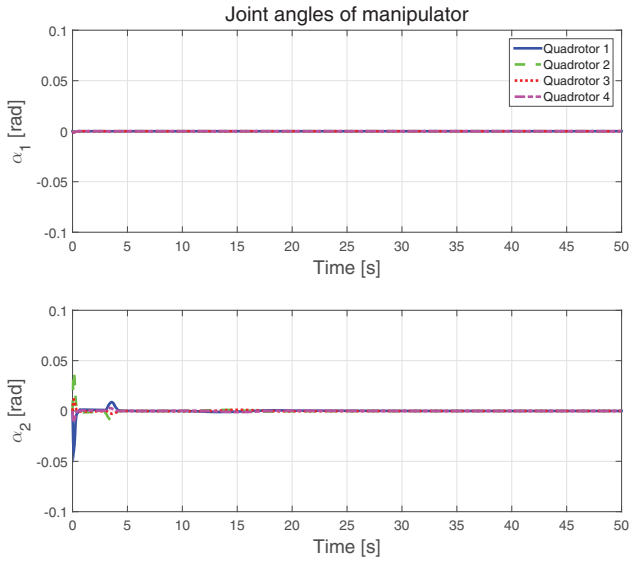


**Figure 8.** Joint angles of the manipulators.

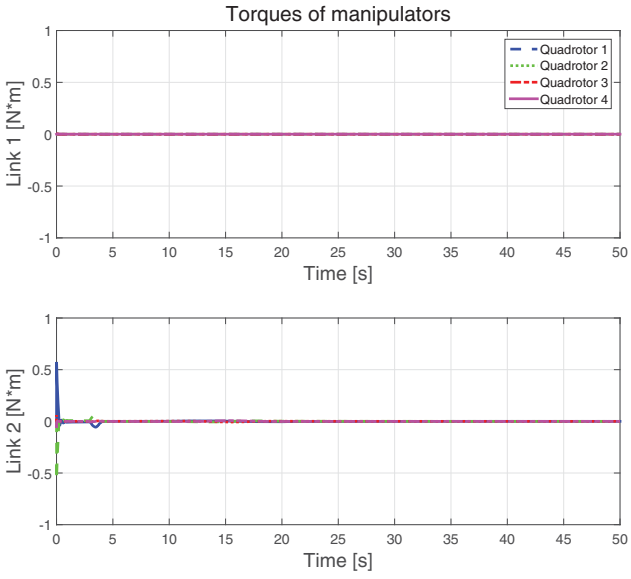


**Figure 9.** Torques of the manipulators.

being avoided. Figure 8 shows the joint angles of the manipulators. When the quadrotors suddenly manoeuvre at the beginning, the manipulators are disturbed. Figure 9 shows the torques history of the manipulators. Figure 10 shows the thrusts history of each rotor of the four quadrotors. All the thrusts are greater than zero and in a reasonable domain, which make sense in the real application.

### 5.2. Example 2 – transporting and assembling task

In this example, let us consider a transporting and assembling task of four quadrotor–manipulator systems. The assembling whole consists of four identical components and each component is a thin square tablet with a 1-m long diagonal. The mass of the component is $m_c = 0.5$ kg. At the beginning, the four quadrotor–manipulator systems carry a component respectively and hover in a line with coordinates $[-4, 0, 5]$, $[-2, 0, 5]$, $[2, 0, 5]$ and $[4, 0, 5]$ m. To achieve the assembling task, the desired formation is a square and the formation offset vectors are designed as $\delta_1 = [-1, 0, 0]$ m, $\delta_2 = [0, 1, 0]$ m, $\delta_3 = [0, -1, 0]$ m and $\delta_4 = [1, 0, 0]$ m. The desired angles of the manipulators are $\alpha_{d,1} = [0, \pi/2]^T$ rad, $\alpha_{d,2} = [-\pi/2, \pi/2]^T$ rad, $\alpha_{d,3} = [\pi/2, \pi/2]^T$ rad and $\alpha_{d,4} = [\pi, \pi/2]^T$ rad. For this problem, we choose $R = 1.5$ m, $r = 0.5$ m. The

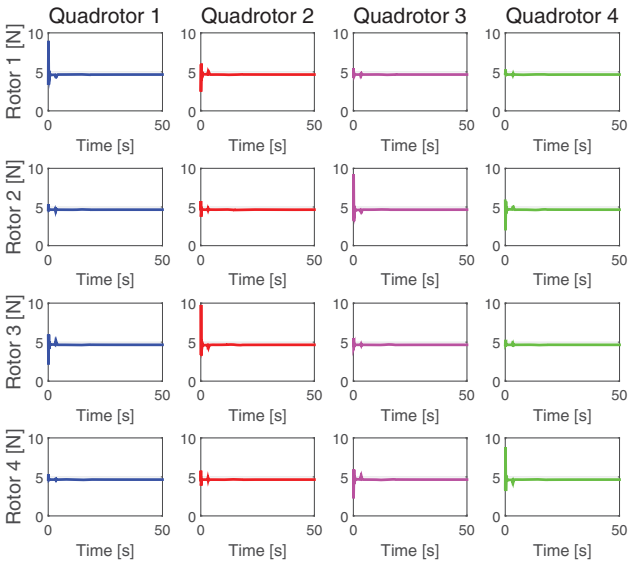


**Figure 10.** Thrusts of each rotor of the four quadrotors.

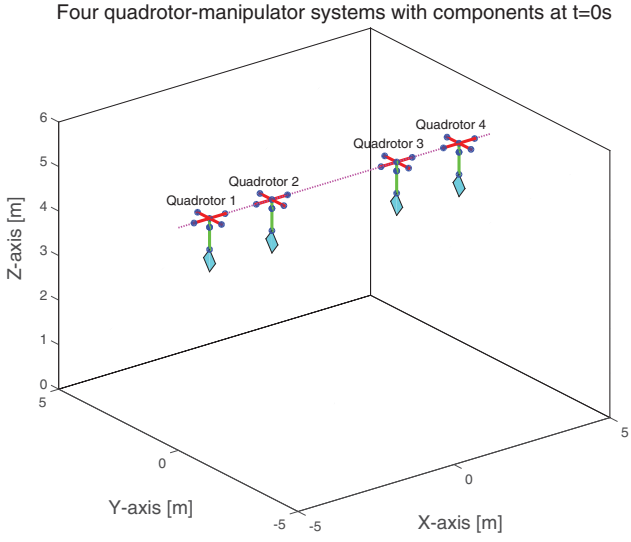


**Figure 11.** The four quadrotor–manipulator systems at $t = 0$ s.

translation and rotation Jacobians of each component are given as follows:

$$J_{P_c} = \begin{bmatrix} -\left(l_2 + \frac{1}{2}d_c\right)\sin(\alpha_1)\sin(\alpha_2) & \left(l_2 + \frac{1}{2}d_c\right)\cos(\alpha_1)\cos(\alpha_2) \\ \left(l_2 + \frac{1}{2}d_c\right)\cos(\alpha_1)\sin(\alpha_2) & \left(l_2 + \frac{1}{2}d_c\right)\sin(\alpha_1)\cos(\alpha_2) \\ 0 & \left(l_2 + \frac{1}{2}d_c\right)\sin(\alpha_2) \end{bmatrix}, \quad (79)$$

$$J_{O_c} = J_{O_2}, \quad (80)$$

where $d_c$ is the length of the component diagonal.

The simulation results are presented in Figures 11–17. We choose the same control gains as Example 1.

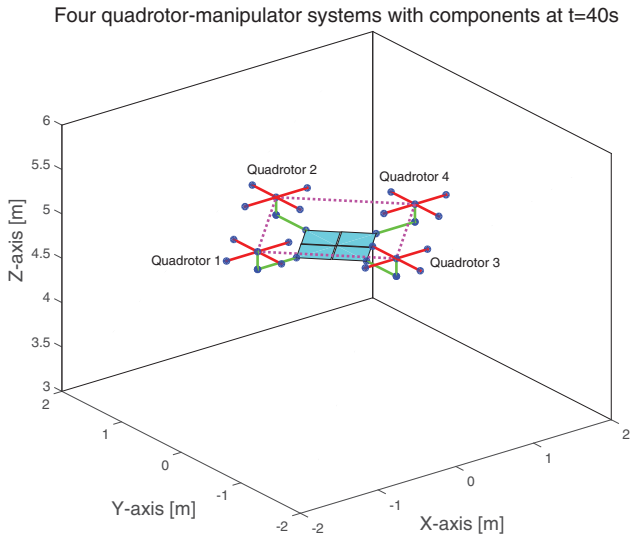


**Figure 12.** The four quadrotor–manipulator systems at $t = 40$ s.

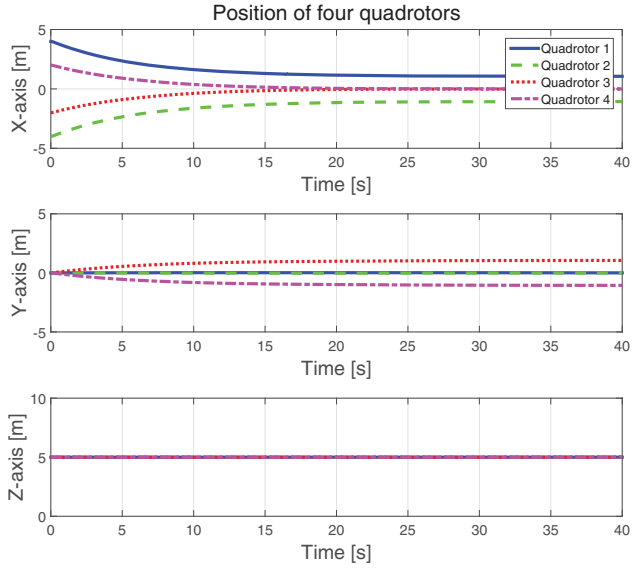


**Figure 13.** Positions of the four quadrotors.

Figure 11 shows the initial status of the four quadrotor–manipulator systems with components which hover in a line. Figure 12 shows that the four quadrotor–manipulator systems with components form the desired formation at $t = 40$ s. The manipulators arrived at the desired positions so that the assembling task is completed.

Downloaded by [Beijing Institute of Technology] at 19:01 11 January 2018

Downloaded by [Beijing Institute of Technology] at 19:01 11 January 2018

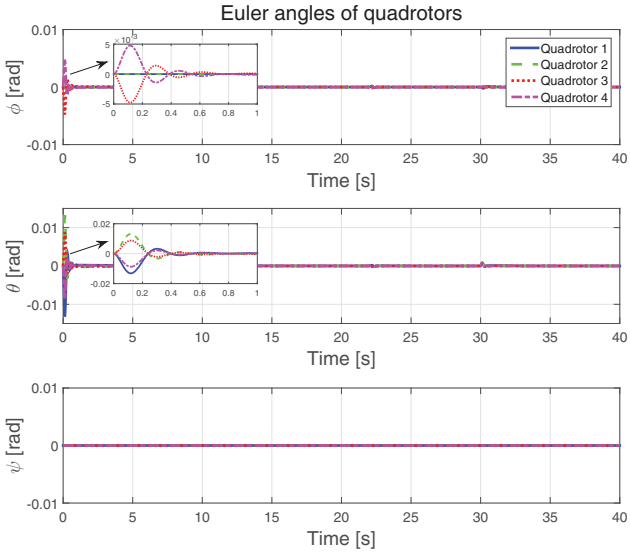


**Figure 14.** Euler angles of the four quadrotors.

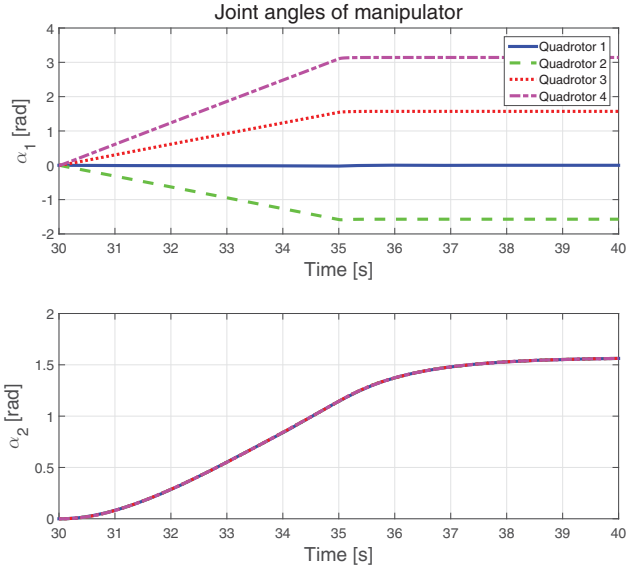


**Figure 15.** Joint angles of the manipulators.

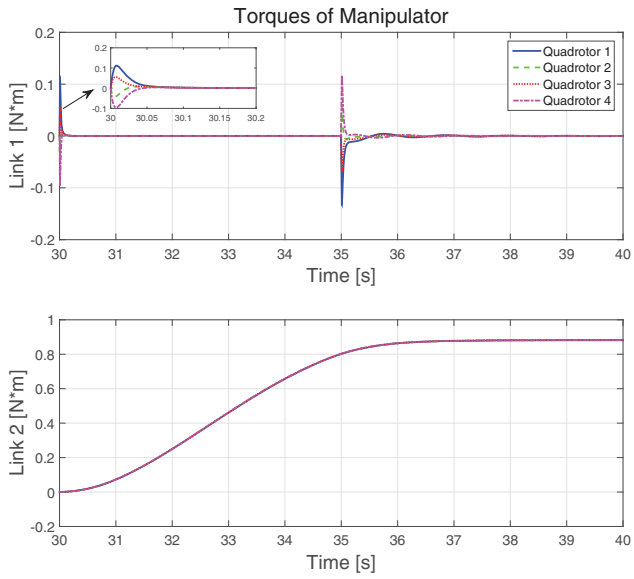


**Figure 16.** Torques of the manipulators.

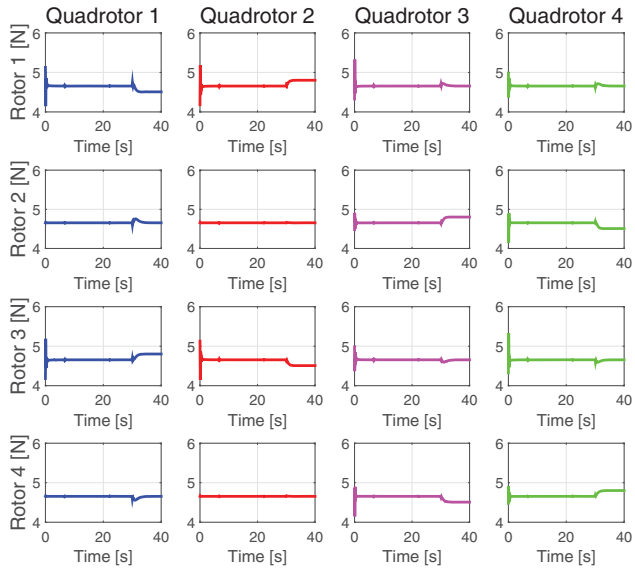


**Figure 17.** Thrusts of each rotor of the four quadrotors.

Figure 13 shows the positions history of the four quadrotors in the $X$, $Y$, $Z$-axes. The formation is achieved when $t$ is greater than 25 s. Figure 14 shows the Euler angles history of the four quadrotors. After the formation has been formed, we start to control the manipulators to the desired position and to finalise the assembling task ($t >$ 30s). Figure 15 shows the joint angles of the manipulators. Figure 16 shows the torques history of the manipulators. Figure 17 shows the thrusts history of each rotor of the four quadrotors.

## 6. Conclusion

In this paper, we present the kinematics and dynamics of quadrotor–manipulator system in a general version handling the quadrotor and the manipulator as an integrated system. To complete the aerial cooperative transporting and assembling task, a control scheme consisting of position controller, attitude controller and manipulator controller is proposed. The proposed position controller is able to achieve formation control and collision avoidance. For attitude stabilisation of the quadrotors, we then propose an attitude controller. A distributed manipulator controller is proposed for tracking the desired joint angles cooperatively. The proposed control algorithm is an important step towards developing the next generation of multiple autonomous quadrotor–manipulator systems. The proposed control scheme is simplified for the real application and the simplified control law is validated by

two formation flying missions of four quadrotors with 2-DOF manipulators. In the future work, it will be interesting to use the directed communication topology, so that the quadrotors can track a desired trajectory in a formation.

## Acknowledgments

The authors highly appreciate the associate editor and reviewer' great efforts in reviewing our manuscript and for providing many helpful comments and suggestions.

## Disclosure statement

No potential conflict of interest was reported by the authors.

## Funding

This work was supported by the National Natural Science Foundation of China [Grant No. 61503025 and 61503333].

## Notes on contributors

***Yuhua Qi*** received his B.S. degree from Beijing Institute of Technology, Beijing China, in 2010. He is currently a Ph.D. candidate at Beijing Institute of Technology. His research interests include cooperative control and autonomous UAV systems.

***Jianan Wang*** is currently an Associate Professor in the School of Aerospace Engineering at Beijing Institute of Technology, Beijing, China. He received his B.S. and M.S. in Control Science and Engineering from the Beijing Jiaotong University and Beijing Institute of Technology, Beijing, China, in 2004 and 2007, respectively. He received his Ph.D. in Aerospace Engineering at Mississippi State University, Starkville, MS, USA in 2011. His research interests include cooperative control of multiple dynamic systems, UAV formation control, obstacle/collision avoidance, trustworthy networked system, and estimation of sensor networks. He is a senior member of IEEE and AIAA.

***Jiayuan Shan*** received the B.S. degree from Huazhong University of Science and Technology in 1988, and the M.S. and Ph.D. degrees from Beijing Institute of Technology, in 1991 and 1999, respectively. He is currently a Professor at Beijing Institute of Technology. His research interests include guidance, navigation and control of the aircraft and hardware-in-the-loop simulation. He is the Director of Department of Flight Vehicles Control and the Deputy Director of Flight Dynamics and Control Key Laboratory of Ministry of Education.

## References

Alonso-Mora, J., Naegeli, T., Siegwart, R., & Beardsley, P. (2015). Collision avoidance for aerial vehicles in multi-agent scenarios. *Autonomous Robots, 39*(1), 101–121.

Arleo, G., Caccavale, F., Muscio, G., & Pierri, F. (2013). Control of quadrotor aerial vehicles equipped with a robotic arm. Proceedings of the 21st Mediterranean Conference on Control & Automation, Platanias-Chania, Crete, Greece (pp. 1174–1180). Greece: IEEE.

Chung, S. J., & Slotine, J. J. E. (2009). Cooperative robot control and concurrent synchronization of Lagrangian systems. *IEEE Transactions on Robotics, 25*(3), 686–700.

Dušan, M. S., Peter, F. H., Mark, W. S., & Dragoslav, D. Š. (2007). Cooperative avoidance control for multiagent systems. *Journal of Dynamic Systems Measurement & Control, 129*(5), 699–707.

Fumagalli, M., Naldi, R., Macchelli, A., & Forte, F. (2014). Developing an aerial manipulator prototype: Physical interaction with the environment. *Robotics & Automation Magazine IEEE, 21*(3), 41–50.

Gioioso, G., Franchi, A., Salvietti, G., & Scheggi, S. (2014). The flying hand: A formation of UAVs for cooperative aerial tele-manipulation. Proceedings of the 21st Mediterranean Conference on Control & Automation, Platanias-Chania, Crete, Greece (pp. 4335–4341). Hong Kong: IEEE.

Graham, A. (1982). *Kronecker products and matrix calculus with applications*. New York, NY: Wiley.

Hokayem, P. F., Stipanović, D. M., & Spong, M. W. (2010). Coordination and collision avoidance for Lagrangian systems with disturbances. *Applied Mathematics & Computation, 217*(3), 1085–1094.

Khalifa, A., Fanni, M., Ramadan, A., & Abo-Ismail, A. (2013, October). Adaptive intelligent controller design for a new quadrotor manipulation system. Proceedings of the 2013 IEEE International Conference on Systems, Man, and Cybernetics, (pp. 1666–1671). Manchester, United Kingdom: IEEE.

Khalil, H. K. (1996). *Nonlinear systems*. NJ: Prentice-Hall.

Kim, S., Choi, S., & Kim, H. J. (2013, November). Aerial manipulation using a quadrotor with a two DOF robotic arm. Proceedings of the 2013 IEEE International Conference on Intelligent Robots and Systems. (pp. 4990–4995). Tokyo, Japan: IEEE.

Lee, H., Kim, H., & Kim, H. J. (2016). Planning and control for collision-free cooperative aerial transportation. *IEEE Transactions on Automation Science & Engineering,* PP(99), 1–13.

Lee, H., & Kim, H. J. (2017). Estimation, control, and planning for autonomous aerial transportation. *IEEE Transactions on Industrial Electronics, 64*(4), 3369–3379.

Mellinger, D., Shomin, M., Michael, N., & Kumar, V. (2013). Cooperative grasping and transport using multiple quadrotors. *Distributed autonomous robotic systems*. Berlin: Springer.

Michael, N., Fink, J., & Kumar, V. (2011). Cooperative manipulation and transportation with aerial robots. *Autonomous Robots, 30*(1), 73–86.

Paden, B., & Panja, R. (1988). Globally asymptotically stable 'PD+' controller for robot manipulators. *International Journal of Control, 47*(6), 1697–1712.

Qi, Y., Wang, J., Jia, Q., & Shan, J. (2016, July). Cooperative assembling using multiple robotic manipulators.

Downloaded by [Beijing Institute of Technology] at 19:01 11 January 2018

Proceedings of the 35th Chinese Control Conference. (pp. 7973–7978). Chengdu, China: IEEE.

Ren, W. (2009). Distributed leaderless consensus algorithms for networked Euler–Lagrange systems. *International Journal of Control, 82*(11), 2137–2149.

Siciliano, B., Sciavicco, L., Villani, L., & Oriolo, G. (2010). *Robotics: Modelling, planning and control*. Berlin: Springer Publishing Company Incorporated.

Thomas, J., Polin, J., Sreenath, K., & Kumar, V. (2013, August). Avian-inspired grasping for quadrotor micro UAVs. Proceedings of the 2013 ASME International Design Engineering Technical Conference. (pp. V06AT07A014–V06AT07A014). Portland, America: American Society of Mechanical Engineers.

Yang, H., & Lee, D. (2014). Dynamics and control of quadrotor with robotic manipulator. Proceedings of the 2014 IEEE International Conference on Robotics and automation (pp. 5544–5549). Hong Kong, China: IEEE.

Downloaded by [Beijing Institute of Technology] at 19:01 11 January 2018